UNCLASSIFIED

AD NUMBER
AD086529
LIMITATION CHANGES

TO:

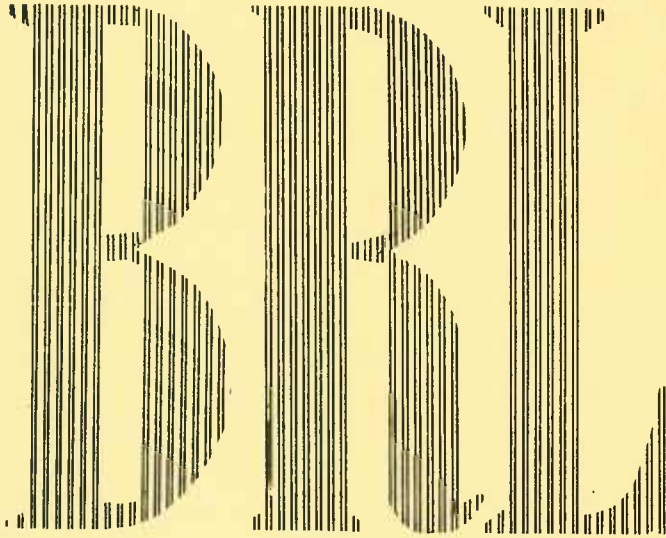Approved for public release; distribution is unlimited.

FROM:

Distribution authorized to U.S. Gov't. agencies and their contractors; Administrative/Operational Use; DEC 1955. Other requests shall be referred to Army Ballistic Laboratory, Aberdeen Proving Ground, MD 21005.

AUTHORITY

usabrl ltr 22 apr 1981

THIS PAGE IS UNCLASSIFIED

BRL

MEMORANDUM REPORT No. 953

DECEMBER 1955

Analog Computer Simulation Of Flight Characteristics Of Two 90MM Fin Stabilized Shell T108E40 And T316

J. M. SCHMIDT

BALLISTIC RESEARCH LABORATORIES

ABERDEEN PROVING GROUND, MARYLAND

BALLISTIC RESEARCH LABORATORIES

MEMORANDUM REPORT NO. 953

DECEMBER 1955

ANALOG COMPUTER SIMULATION OF FLIGHT CHARACTERISTICS
OF TWO 90MM FIN STABILIZED SHELL T108E40 AND T316

J. M. Schmidt

ABERDEEN PROVING GROUND, MARYLAND

TABLE OF CONTENTS

BALLISTIC   RESEARCH   LABORATORIES

MEMORANDUM REPORT NO. 953

JMSchmidt/sdb
Aberdeen Proving Ground, Maryland
December 1955

ANALOG COMPUTER SIMULATION OF FLIGHT CHARACTERISTICS
OF TWO 90MM FIN STABILIZED SHELL T108E40 AND T316

ABSTRACT

A study was made, with the aid of an analog computer, of the effect
of various spin histories upon the dispersion of two 90mm shell, the T108
and T316. The effects of resonance are discussed and graphs illustrating
the motions resulting from several different rates of spin are presented.
A comparison is made between the flight characteristics of the two shell.

TABLE OF SYMBOLS

A	axial moment of inertia of missile
B	transverse moment of inertia of missile
C_1	damping coefficient in roll equation
d	diameter of missile
g	acceleration due to gravity
H	$J_L - J_D + k_2^{-2} J_H$
J_i	$\rho \, d^3 / m \, K_i$
J_ϵ	$\left[i\nu(1 - A/B) \, J_{N_\epsilon} - k_2^{-2} J_{M_\epsilon} \right] \lambda_\epsilon$
k_1	axial radius of gyration $\left(\sqrt{A/md^2} \right)$
k_2	transverse radius of gyration $\left(\sqrt{B/md^2} \right)$
K_3	magnitude of yaw due to asymmetry (function of spin)
K_{3_o}	magnitude of yaw due to asymmetry defined for zero spin
K_D	drag force coefficient $(K_D = K_{D_o} + K_{D_\delta 2} \, \delta^2)$
K_L	lift force coefficient $(K_L = K_N - K_D)$
K_M	overturning (or restoring) moment coefficient
K_{M_ϵ}	asymmetrical moment coefficient
K_N	normal force coefficient
K_{N_ϵ}	asymmetrical normal force coefficient
L	length of missile
ℓ_t	$K_{M_\epsilon} / K_{N_\epsilon}$
m	mass
M	$k_2^{-2} J_M$

p   axial arc length along the trajectory in calibers

S   steady state rolling velocity; also x + iy, swerve

u_o initial velocity of missile

u   velocity of missile $\left(u = u_o\, e^{-\int_o^p J_D\, dp}\right)$

$\bar{u}$ $u_o\, e^{-\int_o^p J_{Do}\, dp}$

x,y,z   positional coordinates in range system in feet

y_G gravity term in swerve equation $\left[\int_o^p \int_o^p gd^2 u^{-2}\, dp\, dp\right]$

α_i damping rates of epicyclic arms

β_i turning rates of epicyclic arms

δ $|\lambda|$

ζ $\zeta_H + i\zeta_V = \lambda/\lambda_t$

Θ $\int_o^p \nu\, dp + \Theta_o$

λ $\lambda_H + i\lambda_V$, the complex yaw

λ_ϵ magnitude of effective asymmetry angle

λ_t trim angle $(k_2^{-2} J_{M_\epsilon} \lambda_\epsilon/M)$

ν_o initial spin of projectile in rad./cal.

ν spin in rad./cal.

$\bar{\nu}$ $(A/B)\,\nu$

ρ density of air

Φ $\alpha_i + i\,\beta_i$

INTRODUCTION

Recent firings of sample groups of the T108E40 shell (Figure 1) in current production indicated extremely poor accuracy in comparison with the accuracy of the same shell during its developmental stages.[1] There naturally arose the problem of determining the causes of this incongruity. The current production shell does not differ significantly in its physical characteristics from its prototype. However, the tail which, during development, was made from aluminum 73ST, is now made from aluminum 63ST, which is known to be weaker. Experimental firings in the Transonic Range showed that the 63ST tail very frequently deforms during launching. These firings also revealed, moreover, that as a result of tail deformation the axial spin and subsequent spin history of this shell in flight varies over a very wide range.

Unfortunately, the nature of this shell is such that it must remain within rather narrow bounds of spin. The upper bound is imposed by penetration requirements and is about 25 RPS; the lower bound is the zone of resonance at about 8 ± 2 RPS. The initial spin is imparted to the shell by the plastic obturating ring and, depending upon the characteristics of this ring, usually lies between 12 and 15 RPS. Normally, the initial spin of $1.9°$/ft. will decay to about $1°$/ft. at 2000 yards, a condition which could be described as satisfactory. In the case of a shell with a deformed tail the normal spin decay might well be accelerated and the shell would approach the resonance condition early in its flight, the resonant spin for this shell being $1.12°$/ft. It was felt that the build-up in the size of the yawing motion which characterizes the resonance phenomenon could have a detrimental effect upon the firing accuracy of the missile.

In connection with this problem a new development came into prominence, namely the 90mm T316 shell (Figure 2). The T316 is a shorter shell with a spiked nose with the result that, at the expense of increased drag, the destabilizing lift on the body of the shell is greatly reduced and the center of pressure of the body is moved closer to the center of gravity of the missile. Therefore, to be stable, this shell requires a relatively

7

short boom. It has no obturating ring and its initial spin is much lower than that of the T108. Since the critical frequency of the T316 is 2.34°/ft., its spin must increase from its initial zero or very low value to a relatively high rate of spin in order to get into resonance. The likelihood of this occurrence is diminished by the fact that, since the shell is quite compact, there is less opportunity for the tail to be damaged as the shell leaves the gun.

This report deals with the investigation, by means of analog computer simulation, of the effects of various spin histories on the trajectories of these two shell. Since resonance appeared to be a possible reason for the poor firing accuracy of the T108E40 shell, particular attention is given to resonance conditions. To this end, six spin histories were arbitrarily assigned to each shell, as shown in the following table.

TABLE 1

SPIN HISTORIES STUDIED

Case	$(d\theta/dz)_0$ (deg./ft.)	$(d\theta/dz)_\infty$ (deg./ft.)	Resonance * Occurs at (yards)
		T108E40	
I,1	0	0	----
I,2	1.9	1.9	----
I,3	1.9	0	(1601)**
I,4	1.9	(-3.2)	500
I,5	1.9	(-0.9)	1000
I,6	1.9	(-0.01)	1500
		T316	
II,1	0	0	----
II,2	1.0	1.0	----
II,3	1.0	0	----
II,4	1.0	(9.8)	500
II,5	1.0	(5.8)	1000
II,6	1.0	(4.4)	1500

* Resonance spin for the T108E40 is 1.12°/ft.; for the T316, 2.34°/ft.

** In the cases I,3 through I,6 and II,4 through II,6 it is seen that from any two conditions the third may be derived. The derived quantities are indicated by parentheses.

Throughout the report the above twelve cases will be referred to as I,1 ..... II,6, wherein the Roman numerals designate the shell and the Arabic numerals the particular spin history under consideration.

The pertinent characteristics of the two shell are given in Table 2 and were obtained experimentally from previous range firings or wind tunnel tests.[1] Note significant differences in drag coefficient, damping rate, pitching frequency, and zero spin trim angle, λ_t,* between the two shell. For example, the T108 trims at 5.07 degrees per degree of tail asymmetry while the T316 trims at 1,83, with the result that the latter shell is much less sensitive to fin deformation.

The following section describes the equations of motion which were programmed for the analog computer.

---

* An aerodynamically asymmetrical shell will assume an equilibrium, or steady state, condition after all transients have died out. The resulting angle of inclination of the geometric axis to the trajectory is the trim angle. It is, in general, a function of spin. The symbol λ_t, used throughout the report, represents the value of the trim angle defined for zero spin.

TABLE 2

PERTINENT CHARACTERISTICS OF 90MM SHELL

	T108E40	T316
L (overall length in cal.)	10.00	6.96
d (diameter in ft.)	.2945	.2945
m (weight in lbs.)	15.60	14.50
c. g. (cal. from base)	3.6	2.98
B (lb.-in.^{2})	727	372.6
A (lb.-in.^{2})	24.3	22.74
$\rho d^3/m$	$1.23(10^{-4})$	$1.32(10^{-4})$
k_2^{-2}	.268	.485
$\left|\ell_t\right|$	5.34	2.92
$\lambda_t/\lambda_\epsilon$	5.07	1.83
Period of yaw (ft.)	322.0	154.0
Pitching frequency (rad./cal.)	.00576	.01203
Damping rate (1/cal.) = H/2	$7.36(10^{-4})$	$1.77(10^{-4})$
u_o(ft./sec.)	2800	2800
C_1 (1/cal.)	$3.24(10^{-5})$	$3.24(10^{-5})$
ν_o (rad./cal.)	$9.76(10^{-3})$	$5.14(10^{-3})$
K_{D_o}	.14	$.22\overset{+}{-}.02$ *
$K_{D_\delta 2}$	$7.07(10^{-4})$	$1.98(10^{-3})$

---

* K_{D_o} is a linear function of Mach number over the Mach number range considered in this problem (see Figure 3). The small Mach number variation of the T108E40 was neglected.

TABLE 2 (continued)

PERTINENT CHARACTERISTICS OF 90MM SHELL

	T108E40	T316
K_N	1.19	1.41
K_{N_ϵ} $(=.8K_N)$	.95	1.13
K_L	1.05	1.10
K_M	-1.00	-2.25
K_{M_ϵ}	-5.07	-4.12

EQUATIONS OF MOTION

If the assumptions of zero initial yaw and zero initial change in yaw are made, and if, further, the very small Magnus and yaw of repose terms are neglected, the linearized differential equation of yawing motion for missiles having slight configurational asymmetry may be written in the following form[2]

$$\lambda'' + (H - i\bar{\nu}) \lambda' - M\lambda = J_\epsilon \, e^{i\Theta} \qquad (1)$$

where primes denote differentiation with respect to p, the axial arc length along the trajectory in calibers. The nomenclature used in the above equation and in the equations to follow is defined in the Table of Symbols preceeding the Introduction.

If the small imaginary term in the expression for J_ϵ is neglected, and if the substitution

$$\lambda_t = \frac{k_2^{-2} \, J_{M_\epsilon} \, \lambda_\epsilon}{M} \qquad (2)$$

is made, equation (1) may be simplified by dividing through by the trim angle, λ_t. Separating the new variable $\lambda/\lambda_t = \zeta$ into its horizontal and vertical components, the equations assume the form in which they were programmed for the analog computer:

$$\zeta_H'' + H\zeta_H' + \bar{\nu}\,\zeta_V' - M(\zeta_H - \cos\Theta) = 0 \qquad (3)$$

$$\zeta_V'' + H\zeta_V' - \bar{\nu}\,\zeta_H' - M(\zeta_V - \sin\Theta) = 0 \qquad (4)$$

The equation of rolling motion for a missile with rotational symmetry may be expressed in terms of the quantities C_1 (damping) and S (steady state rolling velocity) obtained by the present roll reduction technique [3].

$$\nu' = C_1\,(S - \nu) \qquad (5)$$

If all the aerodynamic forces other than the normal force are neglected, the differential equation of swerving motion becomes [2,5]

$$\frac{S''}{d} = \frac{x'' + iy''}{d} = J_L\,\lambda + \frac{M\,e^{i\Theta}\,\lambda_t}{k_2^{-2}\,\left|\ell_t\right|} - \frac{igd}{u^2} \qquad (6)$$

The third term of the above equation, when integrated twice, will be designated by $\dfrac{y_G}{d}$; i.e.

$$y_G = \int_o^p \int_o^p g\,d^2\,u^{-2}\,dp\,dp \qquad (7)$$

The amount of swerve caused by the aerodynamic forces acting on the missile is small in comparison with the drop due to gravity, y_G. Therefore, in order to avoid a scaling problem on the analog computer which would arise if equation (6) were programmed as it stands, it was found convenient to separate the two portions of the equation and plot the resulting motions. One further simplification was made in order to observe the effect of yaw

13

on the gravity term, viz., instead of y_G, a quantity Δy_G was computed such that

$$\Delta y_G = g d^2 \int_o^p \int_o^p (u^{-2} - \bar{u}^{-2})\, dp\, dp \tag{8}$$

where

$$\frac{u'}{u} = -J_{D_0} - J_{D_\delta} 2\, \delta^2 \tag{9}$$

$$\frac{\bar{u}'}{u} = -J_{D_0} \tag{10}$$

Δy_G, then, represents the difference between the gravity drop which occurs when the yaw drag effect is considered and the gravity drop which would obtain at zero yaw.

J_{D_0} is, of course, a function of Mach number. The drag function determined from range firings of the T316 shell is given in Figure 3. The effect of variation in J_{D_0} with Mach number for the Mach number range covered by the T108E40 shell in flight was found to be negligible and hence a constant value of J_{D_0} was employed in equations (9) and (10) when computing the motion of the T108.

Resolving equation (6) (minus the gravity term) into its real and imaginary components, the following quantities are defined:

$$\bar{x}'' = \frac{x''}{d\lambda_t} = J_L\, \zeta_H + \frac{M \cos \Theta}{k_2^{-2}} |\ell_t| \tag{11}$$

$$\bar{y}'' = \frac{y'' + y_G{}''}{d\lambda_t} = J_L\, \zeta_V + \frac{M \sin \Theta}{k_2^{-2}} |\ell_t| \tag{12}$$

Equations (3), (4), (5), (8), (9), (10), (11), and (12) were programmed for the computer. All initial conditions, except v_o' and u_o', were set equal to zero.

14

TABLE 3

Case	Spin History (Cf. TABLE 2)	Yaw History $\lambda_{max.}$* (For λ_ϵ=.2°)	Occurs at Z (yards)	$\sqrt{\bar{x}^2 + \bar{y}^2}$ (mils at 2000 yds.) For λ_ϵ=.2°	Δy_G (mils at 2000 yds.) λ_ϵ=.2°	λ_ϵ=.4°	λ_ϵ=.6°	λ_ϵ=.8°	λ_ϵ=1.0°
I,1	Zero constant spin	1.0	----	38.26	----	----	----	----	----
I,2	Constant spin of 1.9°/ft.	.6	----	.19	----	----	----	----	----
I,3	Zero steady state spin	3.8	1750	.19	.016	.15	.38	.72	1.18
I,4	Resonance at 500 yards	3.6	650	≫ 1	.083	.32	.72	1.30	2.08
I,5	Resonance at 1000 yards	3.7	1200	.19	.025	.25	.63	1.22	2.08
I,6	Resonance at 1500 yards	3.8	1750	.19	.016	.15	.38	.72	1.18
II,1	Zero constant spin	.4	----	5.66	----	----	----	----	----
II,2	Constant spin of 1.0°/ft.	.4	----	.05	----	----	----	----	----
II,3	Zero steady state spin	.4	----	.05	----	----	----	----	----
II,4	Resonance at 500 yards	4.6	700	.05	.68	2.75	7.87	----	----
II,5	Resonance at 1000 yards	6.3	1250	.05	.53	3.50	10.17	----	----
II,6	Resonance at 1500 yards	7.7	1850	.05	.22	.82	2.12	----	----

* For the cases in which resonance does not occur, the values given represent steady state yaw, or magnitude of yaw after transients have damped out. Note that the yaw levels attained by the GEDA in the constant spin cases are verified by the plots of Figure 10.

The quantitative results of the program are presented graphically in Figures 4 through 14 and summarized in Table 3. Some of the qualitative aspects of the program are discussed below.

The graphs representing the various spin histories (Figures 4 and 5) are self-explanatory. Note that the rolling velocity of the T108E40 must decrease in order to reach resonance whereas that of the T316 must increase. Thus it will not be possible to directly compare the cases wherein resonance occurs at 500 yards (I,4 and II,4), for example, since the spin rate of the T108 passes through zero (an undesirable feature, as will presently be shown) while that of the T316 attains a steady state value of 9.8 degrees per foot.

Graphs of the horizontal component [*] of yaw for various spin histories are given in Figures 6, 7, 8 and 9 for a particular degree of "effective asymmetry". The effective angle of asymmetry of a shell is directly related to the trim angle and may be considered to be the asymmetry which produces a trim yaw. This asymmetry may be present due to a variety of causes, such as cocked fins, squashed fins, deformed boom, etc. and is not always measurable prior to firing. It can be inferred from experimental data obtained from a firing by observing the yawing motion at trim and using the following relationship:

$$\lambda_\epsilon = \frac{M\lambda_t}{k_2^{-2} \, J_{M_\epsilon}}$$

(13)

A value of $\lambda_\epsilon = .2^\circ$ was chosen as a representative figure for current manufacturing tolerances and used throughout the program. However, since λ_ϵ appears as a factor in the equations of yawing motion $\left[\text{cf. equations (3) and (4) and recalling that } \lambda/\lambda_t = \zeta\right]$, the magnitude of yaw for other degrees of asymmetry may readily be inferred by applying the appropriate scale to the given graphs.

---

[*] Because of the choice of very special initial conditions ($\lambda = \lambda' = \Theta = 0$), the vertical component of yaw is merely 90° out of phase with the horizontal component after the transients have died out and hence only one component was recorded.

The behavior of the yawing motion undergoing the effects of resonance is of considerable interest. It is seen, by comparison with Figures 4 and 5, that maximum yaw is not attained at the same time that the rolling velocity and pitching frequency are coincidental, but rather at some distance approximately 20% further along the trajectory. Moreover, the maximum amplitude of the resonating yawing motion is a function of the speed with which the spin passes through the resonance region, i.e. the acceleration of the roll angle, Θ. For the cases presented in this report the spin velocity is greatest where resonant spin is reached at 500 yards and least for resonance at 1500 yards. Furthermore, both the T108 and the T316 shell attain the highest yaws when resonant spin is reached at 1500 yards. Thus the more slowly spin passes through the resonance region the greater is the maximum amplitude attained by the yawing motion. The phenomenon, moreover, is more pronounced in the case of the T316 shell; this aspect will be explained by the following discussion.

For constant spin a steady state solution of the form $K_3 \, e^{i\nu p}$ can be assumed for equation (1), and the following relation obtained for the magnitude of K_3:

$$\left| K_3 \right| = \frac{\left[i\nu (1 - A/B) J_{N_\epsilon} - k_2^{-2} J_{M_\epsilon} \right] \lambda_\epsilon}{\left| (1 - A/B)\nu^2 - i\nu H + M \right|} \tag{14}$$

Neglecting the very small contribution of the imaginary term in the numerator of the above expression, the resonance curves for the two shell were calculated for $\lambda_\epsilon = .2^{o}$ and are shown in Figure 10. [*] The abscissa of each point on the curves represents the level of yaw that would be attained for the particular value of (constant) spin indicated as the ordinate of that point. If these two curves are properly used, they are of considerable value in interpreting the yawing motions obtained by the GEDA.

---

[*] In mechanical systems in general, this type of plot, which yields the amplitude, or response, of the system to an external force of any given frequency, is known as a response curve.

It is seen from the graphs that the maximum values of yaw that would be attained by the T108 and the T316 for constant resonant spin are approximately 4° and 12° respectively. The resonant maximum yaw of the T108 shell is, therefore, approximately $(4/.2) \times \lambda_\epsilon$, or in resonance, the shell suffers amplification of its inherent effective asymmetry twenty times. Resonant amplification of the asymmetry of the T316 shell is even larger, being $(12/.2) \times \lambda_\epsilon$, or approximately sixty. The pronounced difference between the peaks of the two curves is due to the difference in damping rates of the two shell, that of the T316 being only about one-fourth the damping rate of the T108 (see Table 2).

A measure of a shell's sensitivity to its trim angle under resonance conditions is given by its magnification factor (m.f.), defined as the ratio of the value of $\left| K_3 \right|$ at resonance spin to the value of $\left| K_3 \right|$ for zero spin (i.e. λ_t). Values of the magnification factor for the T108 and the T316 shell, indicated in Figures 10 and 11, are approximately 4 and 40 respectively.

Figure 11 illustrates the behavior of resonating yawing motion as a function of roll angle acceleration. It consists of two plots [*], representing the T108E40 and the T316 shell, whose coordinates are dimensionless and defined in the following manner:

$$\text{Abscissa:} \quad \frac{\text{Maximum Yaw (ν variable)}}{\left| K_3 \right| \text{ at Resonance}} = \frac{\lambda_{\text{Max.}}}{\left| K_3 \right|_{\text{Reson.}}}$$

$$\text{Ordinate:} \quad \frac{\Delta z}{\text{Period of Yaw}} = \text{Periods of Yaw Near Resonance}$$

where

$$\Delta z = z(\nu_2) - z(\nu_1) \tag{15}$$

$$\nu_1 = .95 \, \nu_{\text{reson.}}$$

$$\nu_2 = 1.05 \, \nu_{\text{reson.}}$$

---

[*] These plots were suggested by C. H. Murphy.

In other words, a "region of resonance", arbitrarily chosen to lie within $\pm$ 5% of critical resonance spin, was marked off and the distance along the trajectory, corresponding to that region, was computed for each of the six resonance cases. This distance, Δz, divided by the period of yaw (see Table 2) becomes the parameter against which the percent of maximum yaw for constant spin, attained along the recorded trajectory, was plotted. (Note that maximum yaw does not necessarily occur within the "region of resonance" as defined in the present discussion.) The results of the two plots are smooth curves which asymptotically approach unity. Moreover, they are suggestive of a family of curves and, since it seemed of some (at least academic) interest, a side program was set up to test that theory. On the order of fifteen additional GEDA runs were made in which the damping coefficient, H, in the yaw equation was allowed to take on different values. Results showed that the two curves given in Figure 11 are indeed members of a family of curves having the magnification factor as the parameter.

Turning, now, from our consideration of the behavior of the yawing motion to the lateral displacement of the shell, and referring once again to the equations which were programmed for the analog computer, it is seen that the vector sum of the motions ($\bar{x}$, $\bar{y}$ and Δy_G) pertaining to the lateral displacement obtained by the simulation process is, in effect, a departure from a particle trajectory rather than the actual trajectory itself. $\bar{x}$ and $\bar{y}$ are the two components of the swerving motion of the shell due to the aerodynamic forces acting upon it; Δy_G is the departure of the shell from a particle trajectory due to increased drag alone. In virtue of very special initial conditions (cf. paragraph following equation 12), $\bar{x}$, the horizontal component, is so small for most of the runs ($\bar{y}$ is greater by a factor of between 20 and 100) as to be negligible and hence the graphical representation of this motion has been omitted from the report. In actual practice, the orientation of the departure of the shell could occur in any plane depending upon the launching conditions.

19

In the preceding paragraph it was stated the for most of the runs $\bar{x}$ is very small. Three exceptions occur: Cases I,1 and II,1 in which the spin rate is identically zero, making the first term in the $\bar{x}''$ equation constant after the transients have died out (the second term is constant by virtue of the zero spin condition) and thereby causing the solution to be almost purely parabolic; and Case I,4, in which the spin rate passes rather slowly through zero at approximately 4000 feet from the beginning of the range. Since, for constant spin, the deflection for missiles having slight configurational asymmetry is proportional to $1/v^2$, it is evident that the condition of zero rolling velocity is to be avoided.

Figure 12 contains plots of $\bar{y}$ for two representative cases. It was found that the passage of the missile through resonance at different places along the trajectory had no appreciable effect upon $\bar{x}$ or $\bar{y}$; i.e., the radius of the helix caused by the yawing motion is negligible in comparison with the jump due to asymmetry. For this reason, the other ten cases are not recorded since, for most of them, the amount of departure is the same as for the two cases shown. Actually $\bar{y}$ for the zero spin cases (I,1 and II,1) is identically zero in virtue of the specific initial conditions of the problem. Case I,4 is also exceptional since $\bar{y}$ becomes very large when the spin rate passes through zero.

All of this information is tabulated in Table 3 under the column headed $\sqrt{\bar{x}^2 + \bar{y}^2}$. The data in this column are the absolute values of the sum of $\bar{x}$ and $\bar{y}$ expressed in mils. Note that the values for the T108E40 are on the order of 25% higher than those for the T316 because of the fact that the T108 has a much higher degree of trim yaw. The effect of the difference in trim angle between the two shell is especially pronounced in the zero spin case wherein it has been shown that the $\bar{x}$ motion is almost purely parabolic. For that case the departure of the T108 is about seven times that of the T316 at a target of 2000 yards. As in the case of the yawing motion, the values given are for an effective asymmetry of $.2^\circ$; for other degrees of asymmetry it is necessary to multiply by the appropriate scale factor.

The remaining data obtained in the program are concerned with the effect due to yaw drag on the gravity term in the swerve equation. Because of the non-linear nature of the equation for y_G, simple scaling of yaw effects is impossible, and computations were made for angles of asymmetry between $.2^O$ and 1^O rather than for one value alone as in the case of the yaw and swerve equations. Since fin distortions of 1^O and even higher have actually been observed on firings of the T108 production shell, the range chosen for this study is realistic. It is felt, however, that by its very nature the T316 is not likely to suffer fin damage of very large magnitude. Indeed, because of the extremely high level of yaw that would be encountered, assumption of as much as 1^O of tail malalignment of the T316 does not permit the use of the Kelley-McShane linearized equations of yawing and swerving motion which are based on the assumption of small yaw. For these reasons, therefore, the study of the yaw drag effect on the T316 was limited to yaws based on $.6^O$ of asymmetry or less.

A few plots of the Δy_G motion (Figures 13 and 14) are presented to show the type of non-linear effect due to yaw drag caused by an increase in yaw level. Note that the amount of deflection at a 1000 yard target is practically insignificant in all cases. However, it is apparent that the deflection at 2000 yards is definitely a function of the place of occurrence of resonance along the trajectory (See also Table 3). If early resonance is avoided, and fin damage remains small, the yaw drag effect, even for the T316 shell, is not too detrimental.

CONCLUSION

In order to summarize the results of the program and draw certain conclusions therefrom, it is worthwhile to review its fundamental objectives. In the introduction an attempt was made to review, at least in part, the history behind the T108E40 and the T316 shell. With this background in mind, then, the problems which emerge from the picture are mainly three

in number:

(1) Does the resonance phenomenon account for the poor firing
accuracy of the T108 shell?

(2) Is the "time of resonance" (place wherein resonance occurs
during flight) significant?

(3) Could the reason for the good accuracy of the T316 shell
be the fact that it is inherently a better shell, from
aerodynamic considerations, than the T108?

Resonance undoubtedly accounts for some of the poor firing accuracy
observed in range firings but its significance appears to be less than
was suspected at the outset of this program. Dispersions of several mils
at 1000 yards, determined experimentally, have not been obtained by the
analog computer study. It appears that the observed behavior of production
lots of the T108 shell has not been simulated since, from this study, the
shell appears to fly very well to a 1000 yard target. At the time of this
writing, an investigation is being conducted [7] to determine the effect on
trajectory of initial yaw and yawing velocity in an effort to explain the
poor firing accuracy of the T108 shell. The results appear promising.

Question two is quite easily resolved from a study of the results
obtained from the analog computer. It is seen (Table 3) that the amount
of displacement due to the aerodynamic forces acting on the shell is not
a function of the place wherein resonance occurs during flight. The
maximum amplitude of the yawing motion does depend upon the "time of
resonance", but this relation is important only when considering its
effect upon the total trajectory. That is to say, the variation of
maximum yaw level with time of resonance is of little more than academic
interest as far as the yawing motion alone is concerned, whereas it has
considerable significance with respect to the amount of displacement due
to yaw drag. Since the drag coefficient is a function of yaw squared,
the relationship of Δy_G to the size of the yawing motion is non-linear

and at 2000 yards its contribution to the total lateral displacement is of considerable magnitude. Nevertheless, at 1000 yards the departure is almost insignificant and hence yaw drag cannot be the explanation for the poor firing accuracy of the production model T108 shell whose dispersions at a 1000 yard target were observed to be on the order of one mil.

Unfortunately, question three cannot be answered unequivocally. A comparison of the aerodynamic properties of the two shell would provide an adequate explanation for the better firing accuracy of the T316 if we had been able to prove that resonance were really the cause of the bad behavior of the T108. In resonance, the T108 shell suffers amplification of its inherent asymmetry twenty times. The tail of this shell is relatively weak, especially if it is made of aluminum 63ST; it is known to suffer considerable deformation during launching on at least 50% of the rounds. The resulting effective asymmetry is often as large as one degree or even larger. Moreover, with relatively low initial spin this shell can get into resonance quite early along its trajectory.

On the other hand, resonant amplification of the T316 shell is considerably larger: it is about sixty times its inherent asymmetry. However, its resonant frequency is approximately 2.34 degrees per foot and starting with zero or very low spin, therefore, it requires a relatively large deformation of the tail to reach resonant spin level within short ranges. Because this shell is more compact, it is likely to launch better, i.e. with less deformation. Hence its chances of reaching resonant spin are much smaller than those of the T108. A comparison of the resonance curves shown in Figure 10 reveals that there is over twice as large a region of spin wherein the T316 will not be near the critical resonance value. Therefore, in this sense it is a better shell, and less likely to experience detrimental effects due to resonance.

The results of this program, although not providing the complete solution to the dispersion problem of the T108 shell, nevertheless shed sufficient light on the situation so as to indicate worthwhile paths for future investigations.

J. M. Schmidt
J. M. SCHMIDT

REFERENCES

1. Karpov, B. G., _Aerodynamic and Flight Characteristics of the 90mm Fin Stabilized Shell, Heat, T108_, BRL Memorandum Report No. 696, July 1953.

2. Murphy, C. H., _Data Reduction for the Free Flight Spark Ranges_, BRL Report No. 900, February 1954.

3. Bolz, Ray E. and Nicolaides, J. D., _A Method of Determining Some Aerodynamic Coefficients from Supersonic Free Flight Tests of a Rolling Missile_, BRL Report No. 711, November 1949.

4. Murphy, C. H., _On Stability Criteria of the Kelley-McShane Linearized Theory of Yawing Motion_, BRL Report No. 853, April 1953.

5. Nicolaides, J. D., _On the Free Flight Motion of Missiles Having Slight Configurational Asymmetries_, BRL Report No. 858, June 1953.

6. Karpov, B. G., and Piddington, M. J., _Effect on Drag of Two Stable Flow Configurations Over the Nose Spike of the T316 Projectile_, BRL TN 955.

7. Simon, W. E., _Investigation of the Causes of High Dispersion of the Production 90mm Fin-Stabilized Shell, HEAT, T108E40_, BRL Memorandum Report No. 967, February 1955.

1. Photograph of T108E40

2. Photograph of T316

3. Drag Function of T316 (K_{D_o} vs. Mach Number)

4. $\emptyset'$ vs Z for T108E40

5. $\emptyset'$ vs Z for T316

6. λ_H vs Z for T108E40 (cases I,1; I,2; and I,3)

7. λ_H vs Z for T108E40 (cases I,4; I,5; and I,6)

8. λ_H vs Z for T316 (cases II,1; II,2; II,3; and II,5)

9. λ_H vs Z for T316 (cases II,4 and II,6)

10. Resonance Curves (K_3 vs. Spin)

11. $\lambda_{max.}$ vs. ΔZ

12. $\bar{y}$ vs. Z (cases I,5 and II,5)

13. Δy_G vs. Z for T108E40

14. Δy_G vs. Z for T316
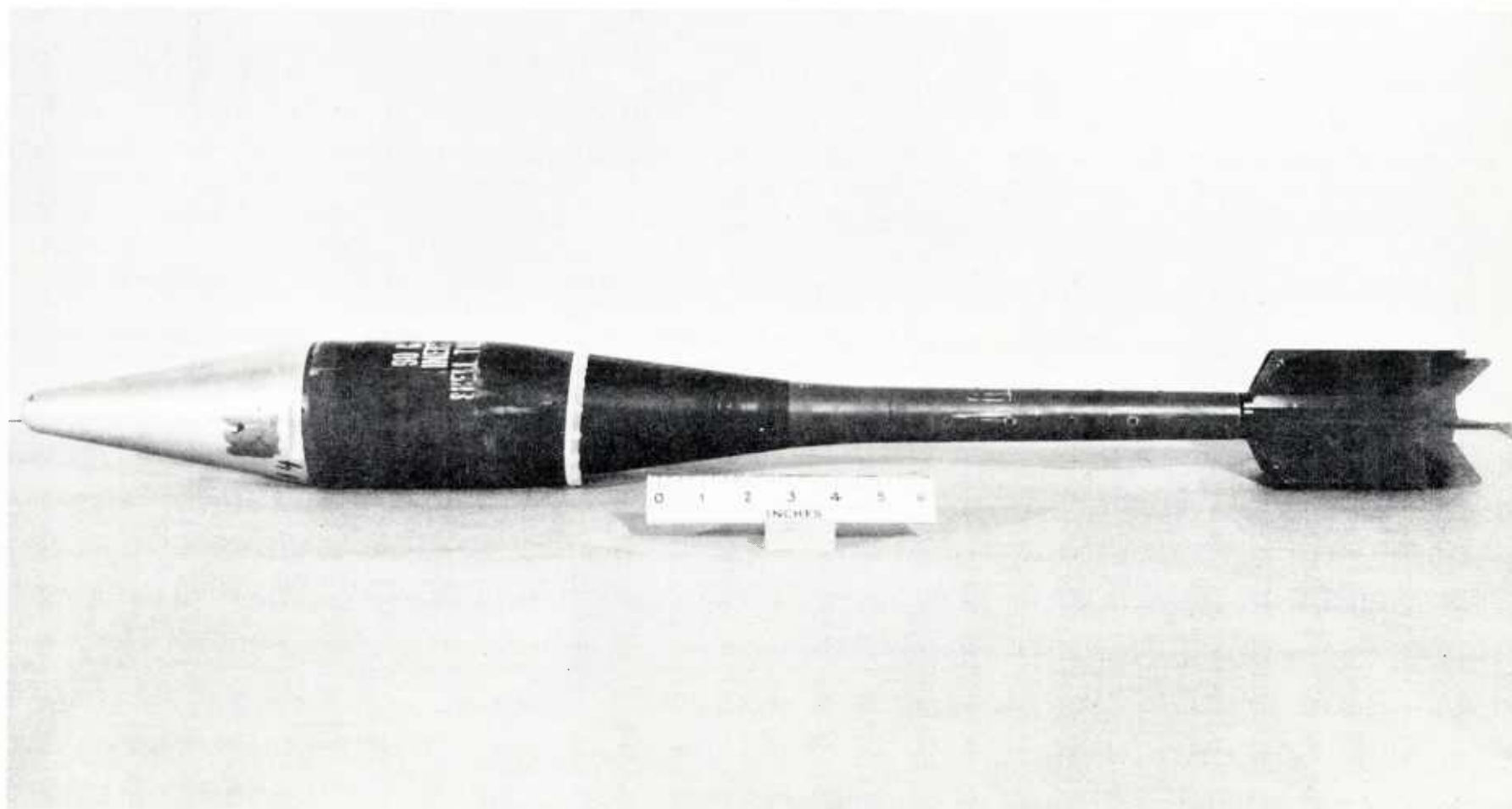
T108   E40

FIG. 1

T316

FIG. 2

K_{D_o} vs MACH NUMBER

T 316
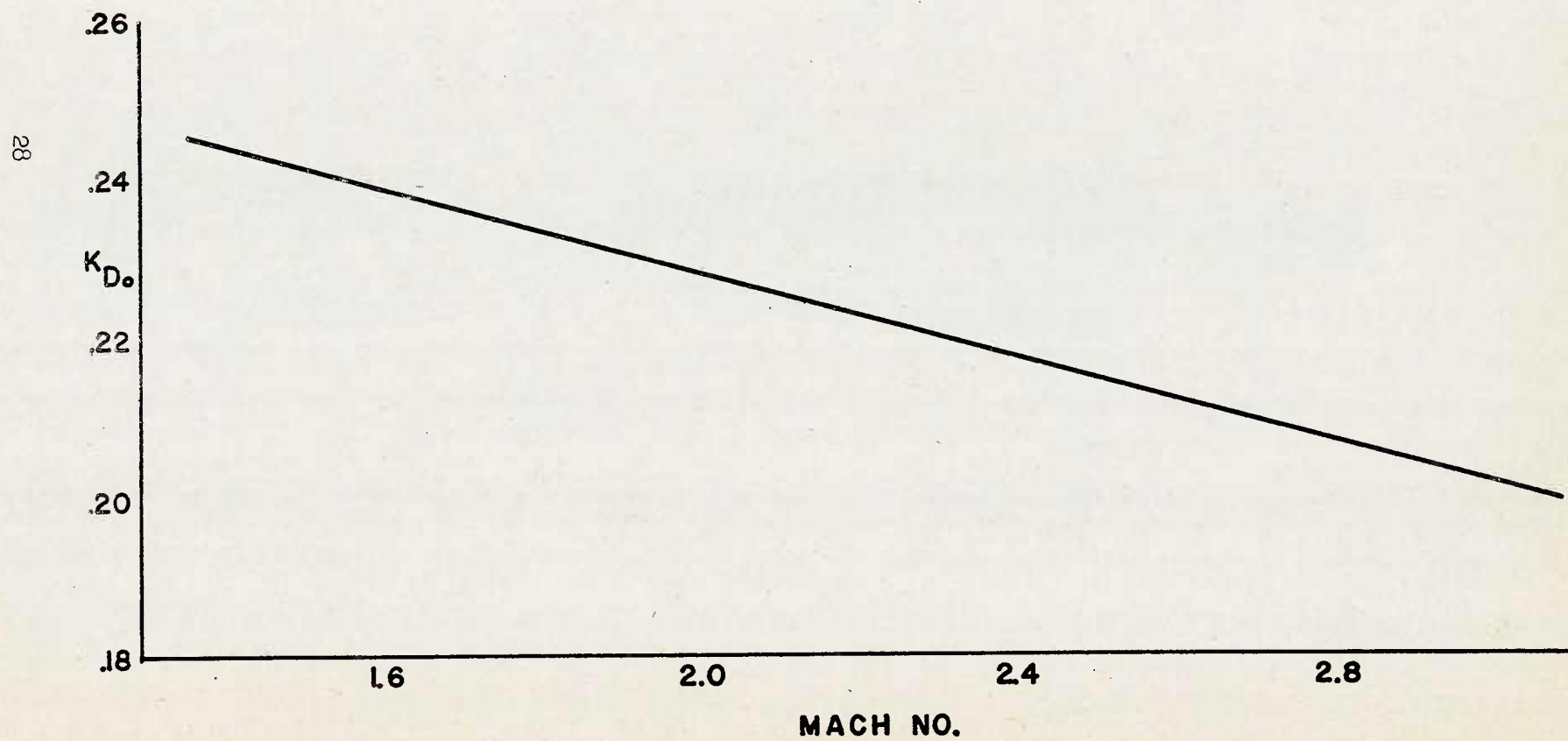
FIG. 3

$\dfrac{d\theta}{dz}$ (SPIN in deg/ft)
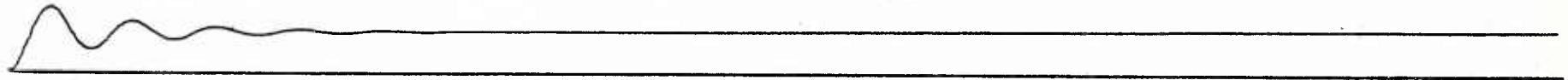
vs

Z (DISTANCE in yards)

T 108 E 40
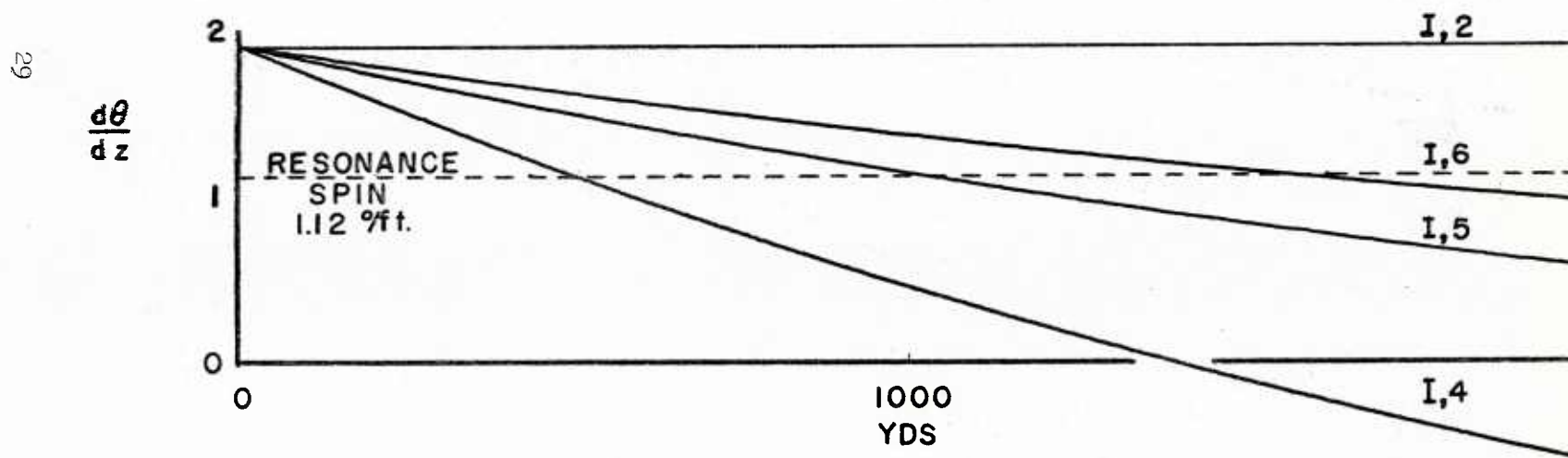
FIG. 4
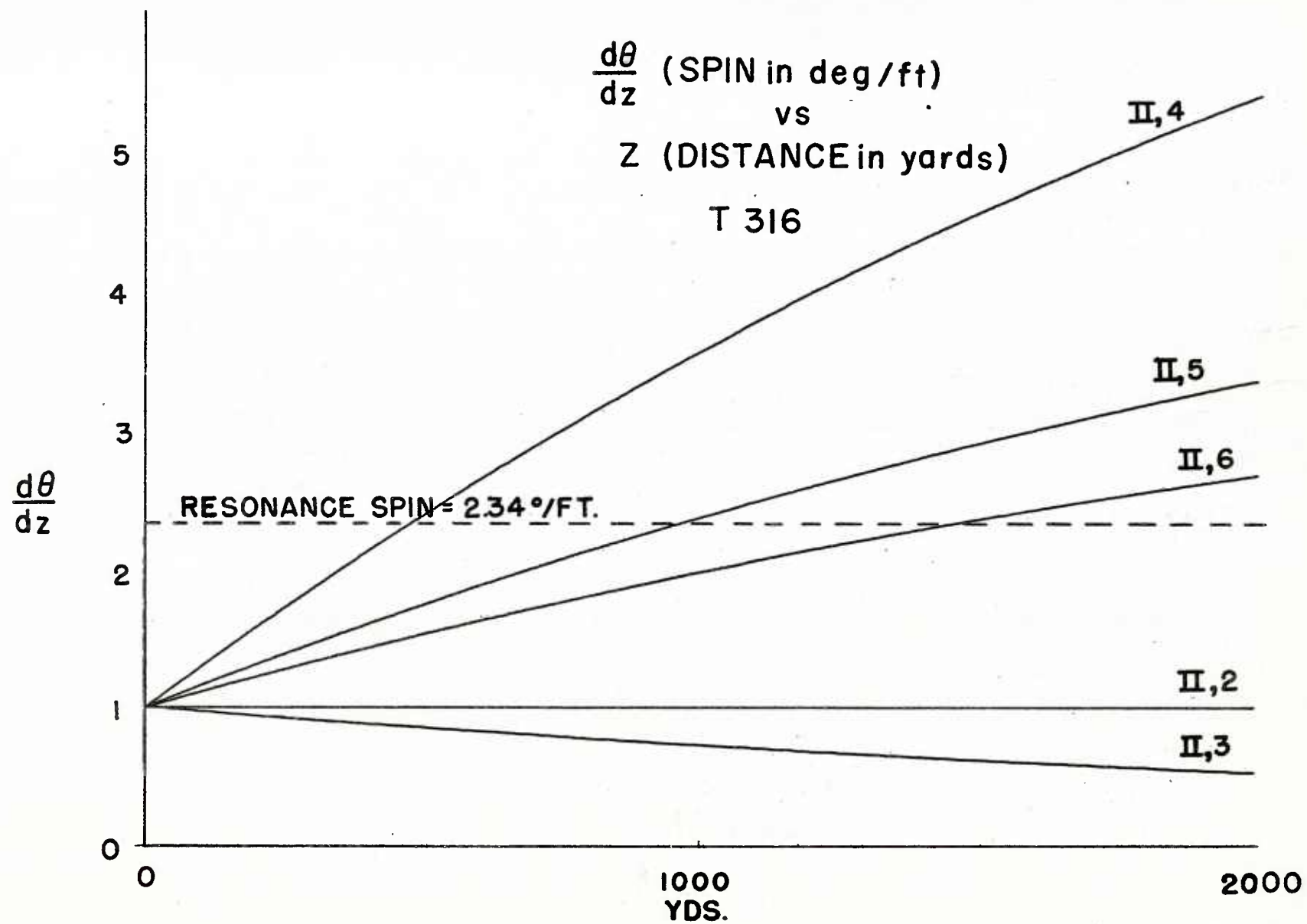
$\frac{d\theta}{dz}$ (SPIN in deg/ft)

vs

Z (DISTANCE in yards)

T 316

5

4

3

$\frac{d\theta}{dz}$

RESONANCE SPIN = 2.34°/FT.

2

1

0

0

1000
YDS.

2000

II,4

II,5

II,6

II,2

II,3

30

FIG. 5

λ_H(deg) vs Z (yards)
FOR λε = .2°
T108 E 40
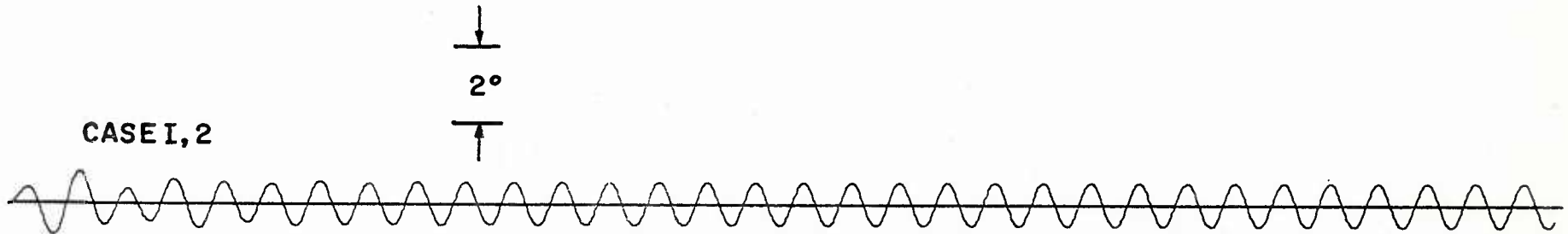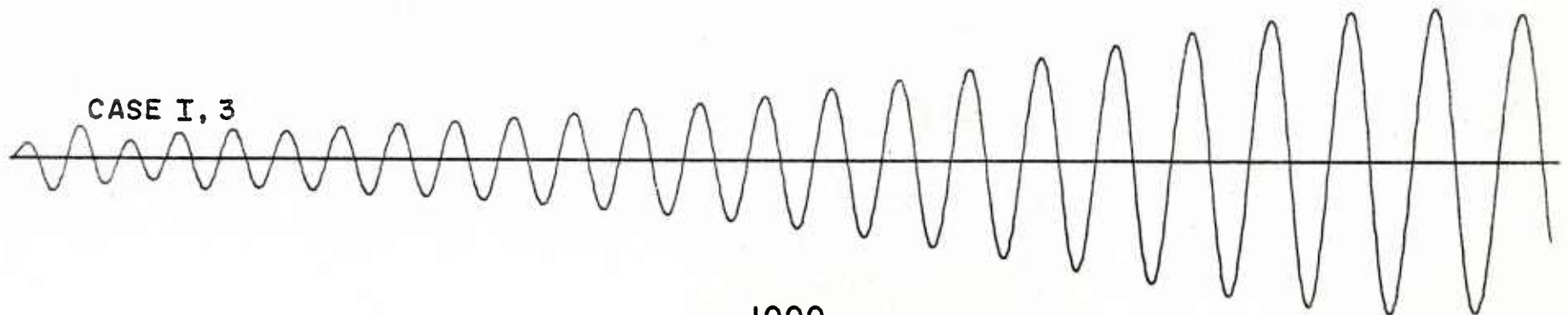
FIG. 6

λ_H (deg) vs Z (yards)
FOR λ_ε = .2°
T 316
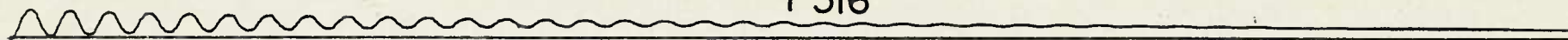
CASE II, I

CASE II, 2

CASE II, 3

2°

CASE II, 5

1000

FIG. 8

33
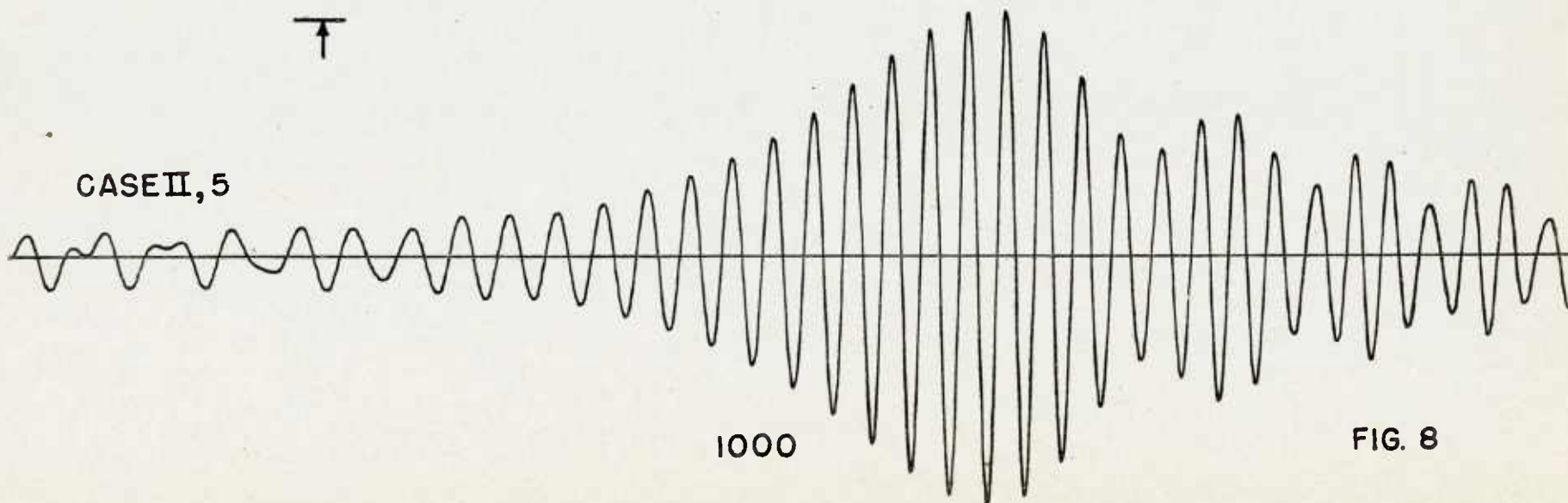
$\lambda_H(deg)$ vs Z (yards)
FOR $\lambda \epsilon = .2°$
T 316

2°

CASE II, 4
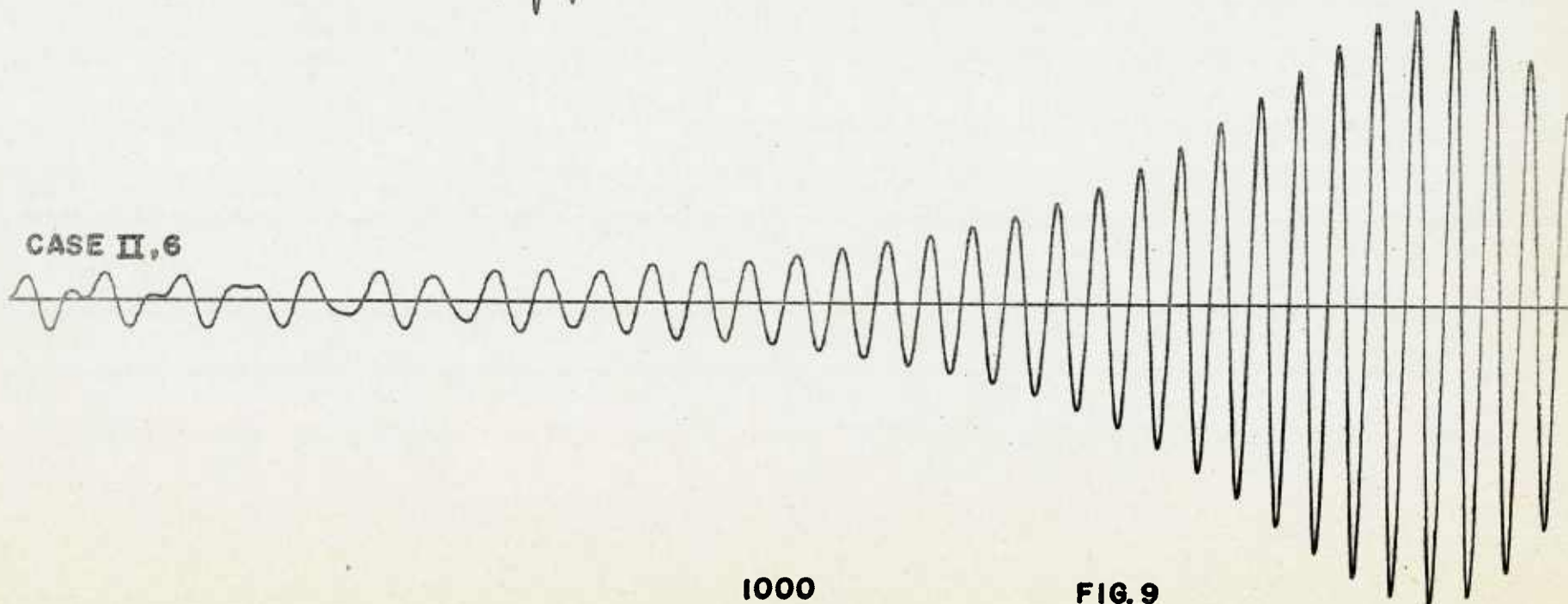
CASE II, 6

1000   FIG. 9

34
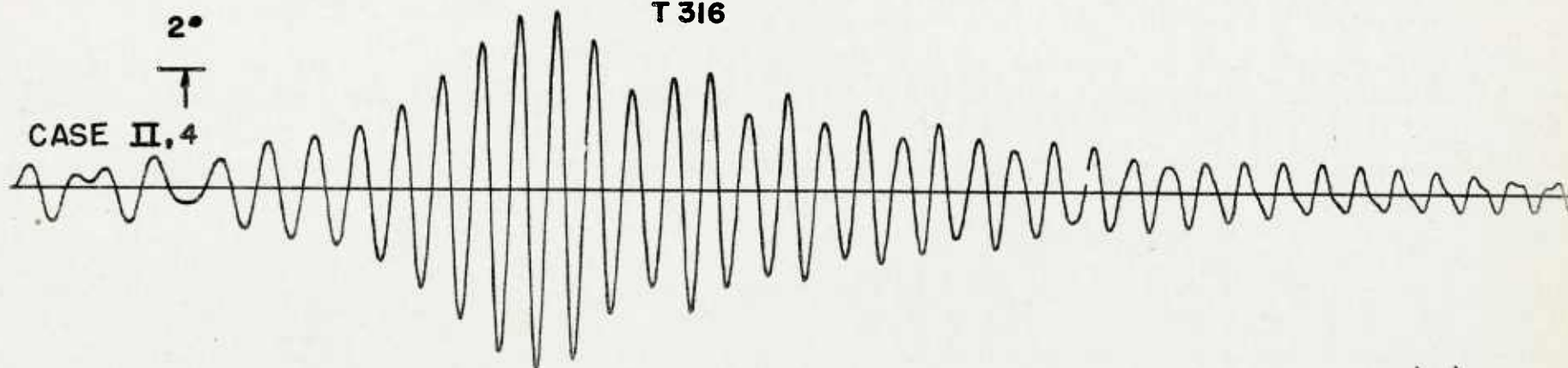
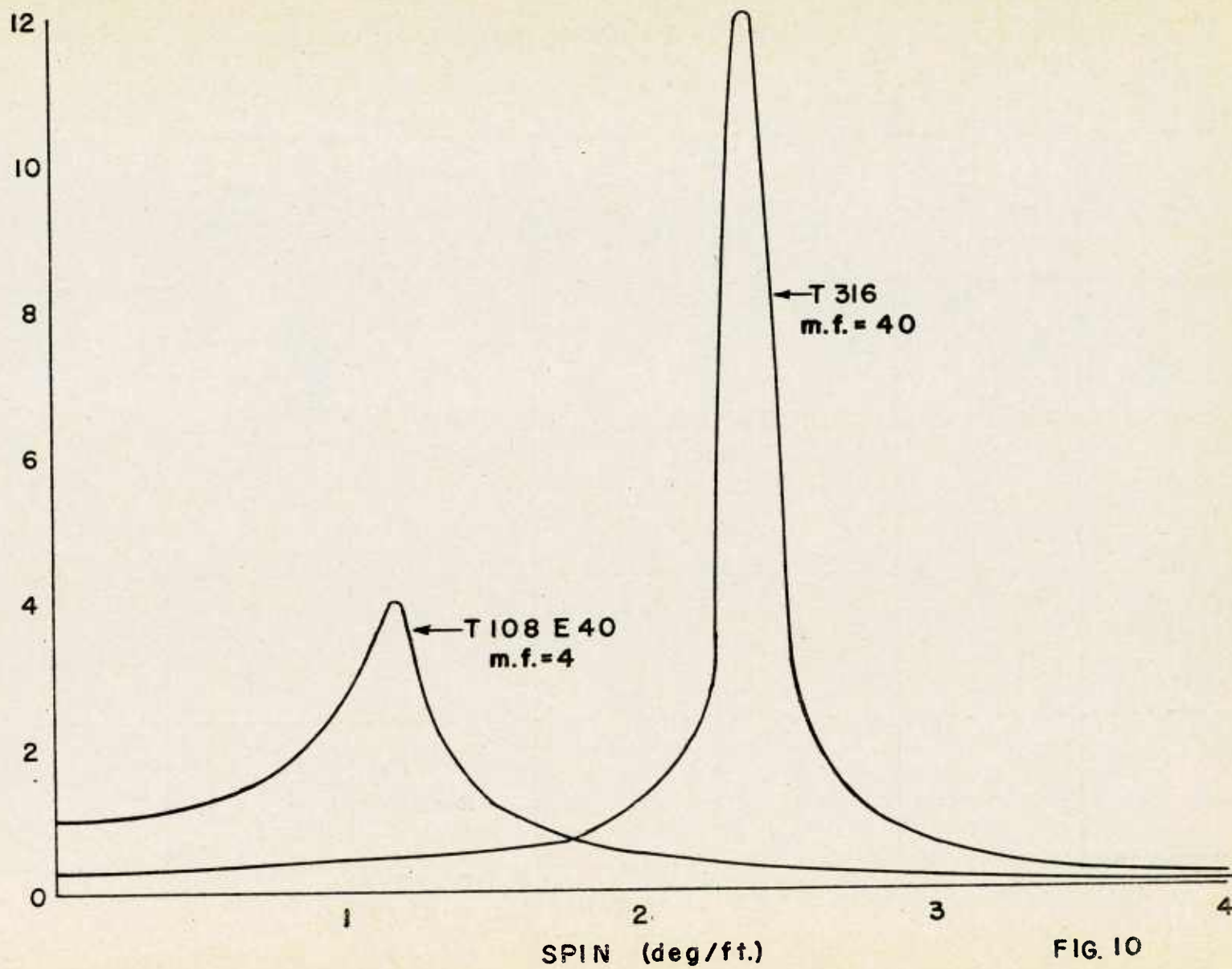$|K_3|$ (FOR $\lambda\epsilon = .2°$)   vs.   SPIN

FIG. 10
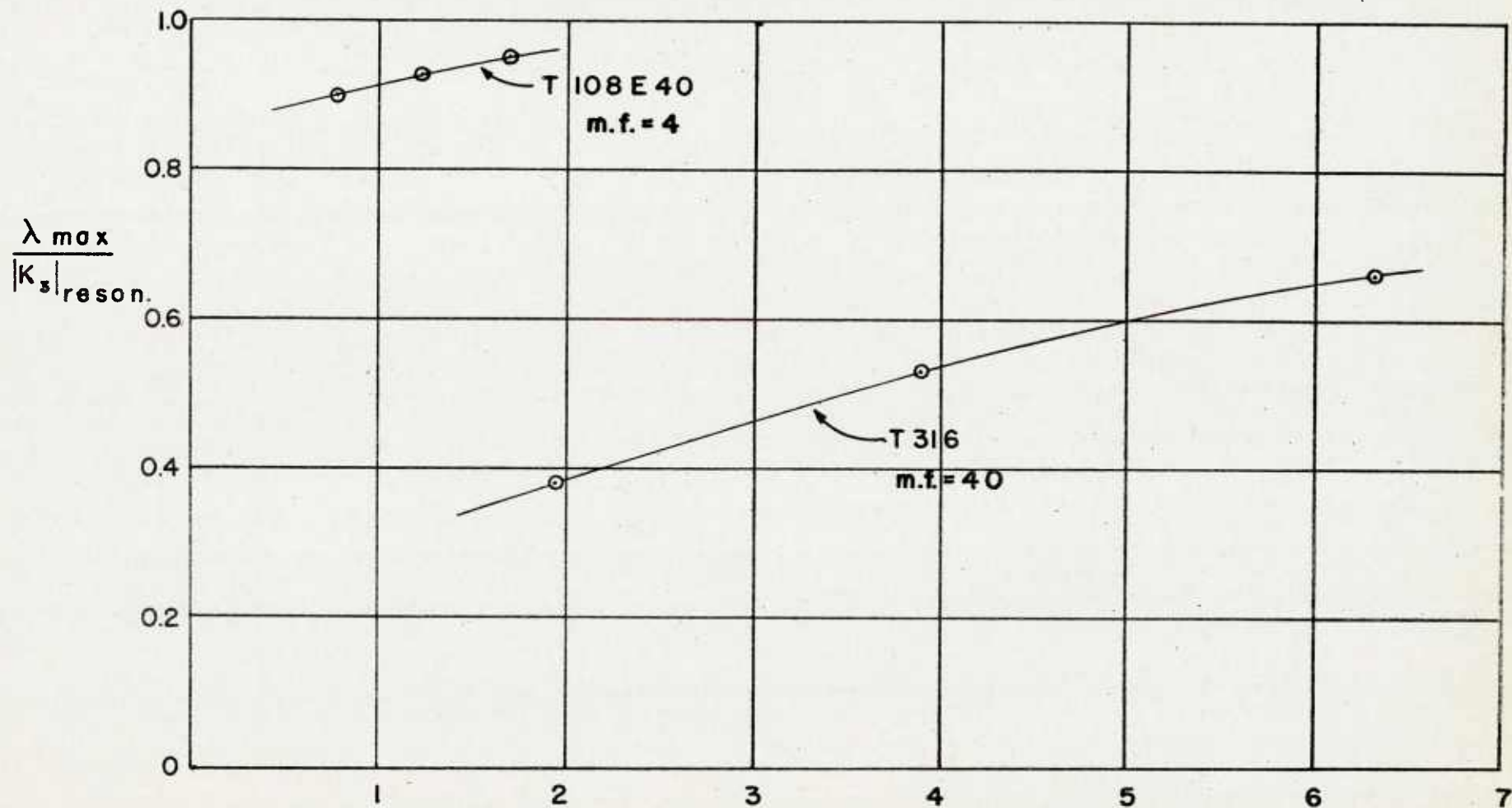
PERIODS OF YAW NEAR RESONANCE

$.95\nu_{reson.} < \nu < 1.05\nu_{reson.}$

FIG. 11

$\overline{Y}$ vs Z
(CASES I,6 and II,6)

T 108 E 40

T 316

$\overline{Y}$

1.0

.8

.6

.4

.2

0

37

1000
YDS.

FIG. 12

ΔY_G vs Z

T 108 E 40

CASE I, 4

$J_{D_0} = 1.722 \times 10^{-5}$

$J_{D\lambda^2} = 8.69 \times 10^{-8}$

FIG 13

ΔY_G vs Z

T 316

CASE II,4

$J_{D\chi^2} = 2.61 \times 10^{-7}$

$\lambda_\epsilon = .6°$

$\lambda_\epsilon = .4°$

$\lambda_\epsilon = .2°$

YDS
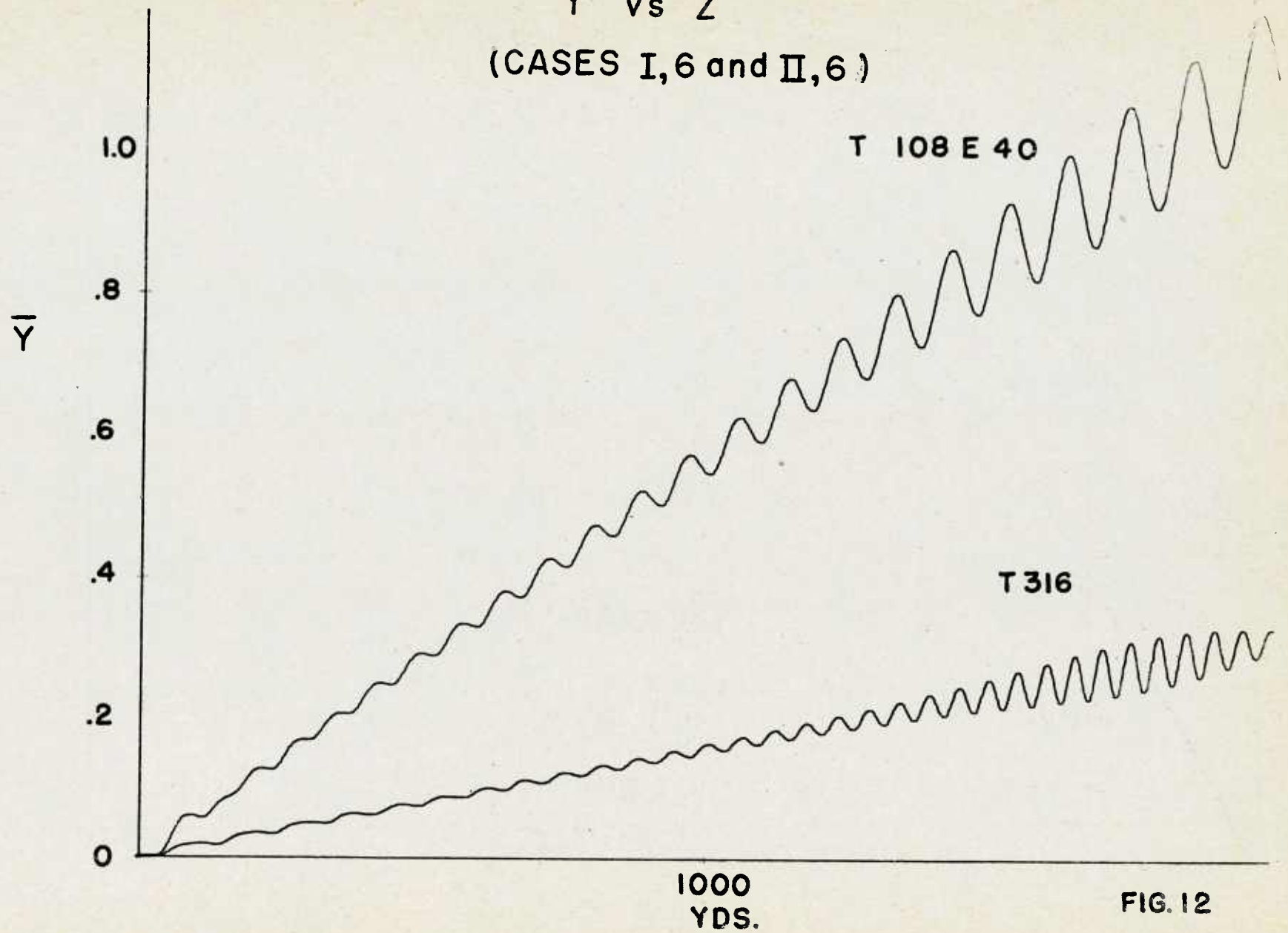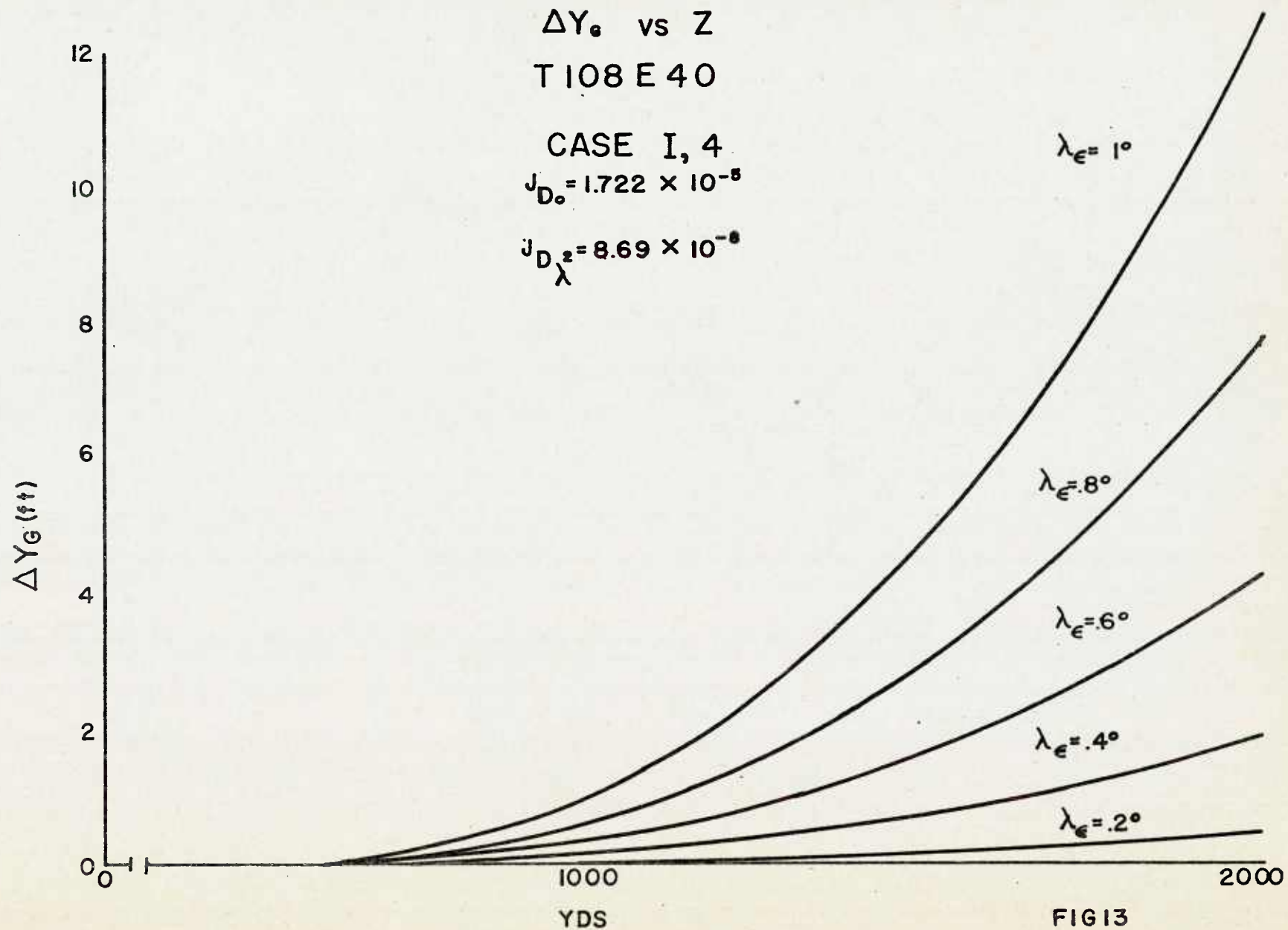
FIG 14

APPENDIX: COMPUTER CHECK SOLUTIONS

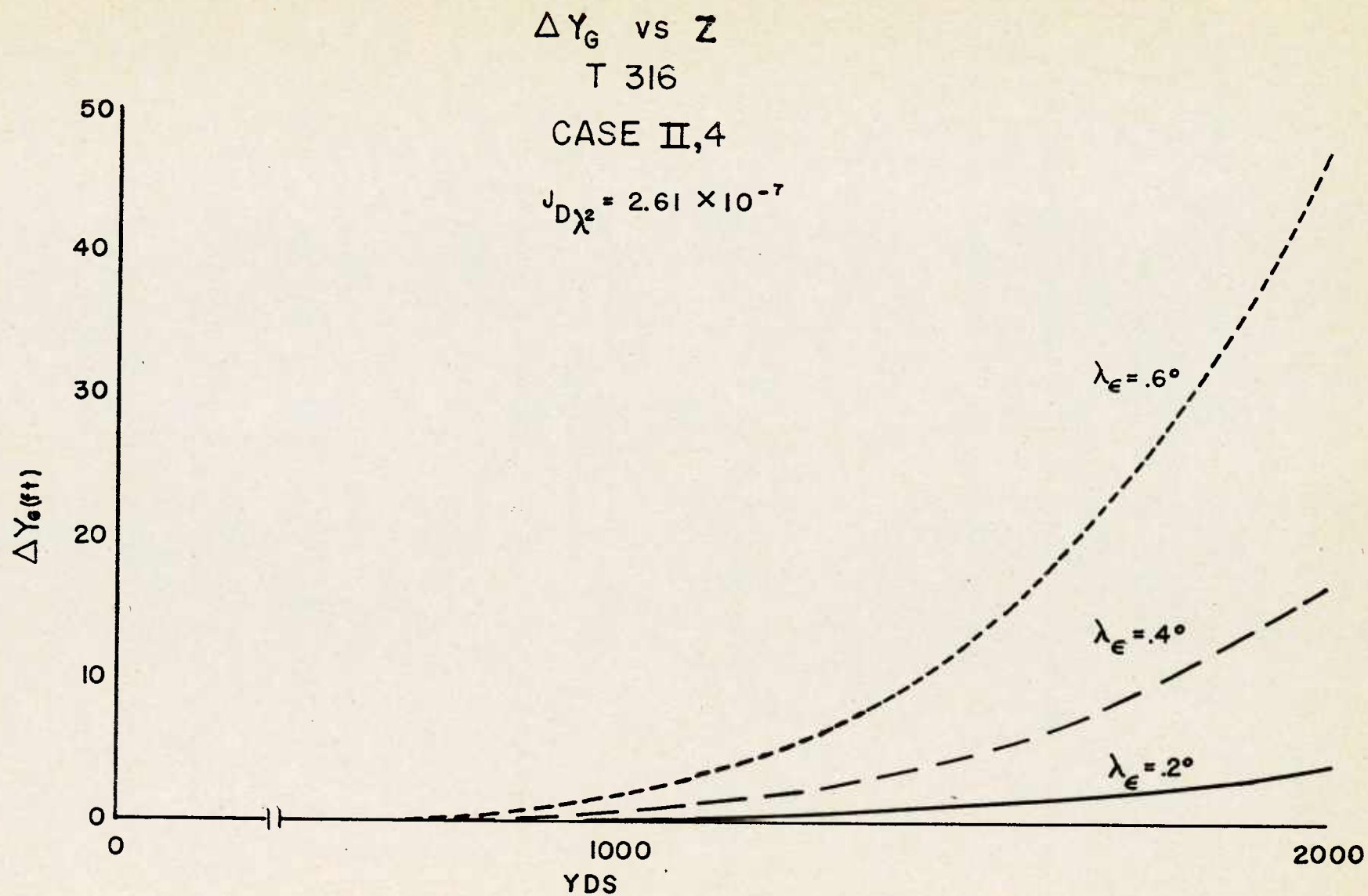Several special runs were made on the computer for the purpose of checking the validity of the solutions being obtained. They were arranged so as to check, as nearly as possible, all of the parts of the circuit.

When the rolling velocity of the missile is constant, the solution to the differential equations of yawing and swerving motion may be written exactly in terms of simple functions, thereby permitting a fairly simple check of the computer solution for constant spin. These equations are [2,5]

$$\lambda = \sum_{i=1}^{3} K_i\, e^{\Phi_i p} \tag{16}$$

and

$$\frac{x + iy}{d\lambda_t} = J_L \sum_{i=1}^{3} \frac{K_i(e^{\Phi_i p} - 1 - \Phi_i p)}{\lambda_t} +$$

$$\left[\frac{M}{k_2{}^{-2}\,|\ell_t|} \right] \left[\frac{e^{\Phi_3 p} - 1 - \Phi_3 p}{\Phi_3{}^2} \right], \tag{17}$$

the gravity term having been omitted from the present discussion. With the assumption of zero initial yaw and zero initial change in yaw,

$$K_1 = \frac{K_3(\Phi_2 - \Phi_3)}{\Phi_1 - \Phi_2} \tag{18}$$

$$K_2 = \frac{-K_3(\Phi_1 - \Phi_3)}{\Phi_1 - \Phi_2} \tag{19}$$

$$K_3 = \frac{\left[iv(1 - A/B)\, J_{N_\epsilon} - k_2{}^{-2}\, J_{M_\epsilon} \right]\lambda_\epsilon}{(\Phi_1 - \Phi_3)\,(\Phi_2 - \Phi_3)} \tag{20}$$

$$\Phi_1 = -\alpha_1 + i\,\beta_1 \tag{21}$$

$$\Phi_2 = -\alpha_2 + i\,\beta_2 \tag{22}$$

$$\Phi_3 = i\nu \tag{23}$$

The spin, ν, may be chosen arbitrarily for this computation, while α_i and β_i, the damping rates and turning rates, respectively, of the two epicyclic arms, are specified by the equations

$$\Phi_1 \cdot \Phi_2 = -M \tag{24}$$

$$\Phi_1 + \Phi_2 = -H + i\,\bar{\nu} \tag{25}$$

λ_t, the trim angle, or magnitude of yaw due to asymmetry after the transients have died out, is given approximately by

$$\lambda_t = \frac{k_2^{-2}\, J_M\, \lambda_\epsilon}{M} \;. \tag{26}$$

Neglecting the very small imaginary term in equation (20), K_3 may then be rewritten in terms of the trim angle, λ_t:

$$\frac{K_3}{\lambda_t} = \frac{-M}{(\Phi_1 - \Phi_3)(\Phi_2 - \Phi_3)} \tag{27}$$

If the constant and linear terms of equation (17) are designated as $P/d\lambda_t$ and $Q/d\lambda_t$, respectively, where P and Q are complex, then

$$\frac{P}{d\lambda_t} = -\frac{J_L}{\lambda_t} \sum_{i=1}^{3} \frac{K_i}{\Phi_i^2} + \frac{M}{k_2^{-2}\,\nu^2}\left|\ell_t\right| \tag{28}$$

$$\frac{Q}{d\lambda_t} = -\frac{J_L}{\lambda_t} \sum_{i=1}^{3} \frac{K_i}{\Phi_i} + \frac{M}{k_2^{-2}\,\nu}\left|\ell_t\right| \tag{29}$$

Since the remaining terms of the swerve equation are oscillatory in nature, it is necessary to compute only $(P_1 + Q_1 p)$ and $(P_2 + Q_2 p)$ in order to determine the horizontal (x) and vertical (y) displacements at some given distance, p, in calibers along the trajectory. With the following data as input,

$$\nu \quad = 5.14 \times 10^{-3} \text{ rad./cal.}$$

$$H \quad = 1.4725 \times 10^{-3}$$

$$M \quad = -.32964 \times 10^{-4}$$

$$\lambda_t \quad = 1.104$$

$$d \quad = .2945 \text{ ft.}$$

the necessary quantities for solving equations (28) and (29) were computed, with the result that at p = 20373.5 cal. (2000 yards)

	HAND COMPUTATION	COMPUTER SOLUTION
x	.028 ft.	.03 ft.
y	2.173 ft.	2.13 ft.

In order to obtain a check solution of the gravity term in the equation of swerving motion, a constant drag coefficient was assumed, thus permitting the direct formal integration of the expression for y_G. Thus, for constant J_D,

$$y_G = gd^2 \int_0^p \int_0^p u^{-2} \, dp \, dp = gd^2 u_0^{-2} \left\{ \frac{e^{2J_D p} - 2J_D p - 1}{(2J_D)^2} \right\} \quad (30)$$

where $u = u_0 e^{-J_D p}$.

With the following data as input,

$$u_o = 2800 \text{ ft./sec.}$$

$$g = 32.16 \text{ ft./sec.}^2$$

$$d = .2945 \text{ ft.}$$

$$J_D = 4.848 \times 10^{-5}$$

$$p = 20373.5 \text{ cal.}$$

a hand computation of the quantity y_G was made and compared with the analog computer solution with the result that

	HAND COMPUTATION	COMPUTER SOLUTION
u	1042.8 ft./sec.	1040.3 ft./sec.
Y_G	160.12 ft.	161.00 ft.

A similar procedure was followed to check the inclusion of the yaw drag term. A constant average value of yaw squared of 4 square degrees was assumed, and the velocity equation was permitted to take the form

$$u = u_o \, e^{-J_D p}$$

where $J_D = J_{D_o} + J_{D_\delta 2} \, \delta^2$ and $J_{D_\delta 2} = 2.608 \times 10^{-7}$. A non-linear unit of the analog computer was used to compute $J_{D_\delta 2} \, \delta^2$, even though for this computation all the quantities are constant, in order to simulate as closely as possible the actual requirements of the problem when the yawing motion is not constant. Results again indicated a fairly high degree of accuracy for the analog computer solution.

	HAND COMPUTATION	COMPUTER SOLUTION
y_G	156.9 ft.	157.2 ft.

DISTRIBUTION LIST

No. of Copies	Organization	No. of Copies	Organization
	Chief of Ordnance Department of the Army Washington 25, D. C. Attn: ORDTB - Bal Sec	1	Commander Naval Air Development Center Johnsville, Pennsylvania
		2	Commander Naval Ordnance Test Station China Lake, California Attn: Technical Library
10	British Joint Services Mission 1800 K Street, N. W. Washington 6, D. C. Attn: Mr. John Izzard Reports Officer	1	Commanding Officer & Director Naval Research Laboratory Washington 25, D. C. Attn: W. A. McCool (Code 6231)
4	Canadian Army Staff 2450 Massachusetts Avenue Washington 8, D. C.	4	Commanding General Air Research & Development Command P. O. Box 1395 Baltimore 3, Maryland Attn: Deputy for Development
3	Chief, Bureau of Ordnance Department of the Navy Washington 25, D. C. Attn: Re3	3	Director National Advisory Committee for Aeronautics 1512 H Street, N. W. Washington 25, D. C.
2	Commander Naval Proving Ground Dahlgren, Virginia		

2	Commander
	Naval Ordnance Laboratory
	White Oak
	Silver Spring, Maryland
	Attn: Mr. Nestingen
	    Dr. May
		1	Director
			National Advisory Committee
			  for Aeronautics
			Ames Laboratory
			Moffett Field, California
			Attn: Dr. A. C. Charters
			    Mr. H. J. Allen

1	Superintendent
	Naval Postgraduate School
	Monterey, California
		3	National Advisory Committee
			  for Aeronautics
			Langley Memorial Aeronautical
			  Laboratory
			Langley Field, Virginia
			Attn: Mr. J. Bird
			    Mr. C. E. Brown
			    Dr. Adolf Busemann

2	Commander Naval Air Missile Test Center Point Mugu, California		
1	Commanding Officer and Director David W. Taylor Model Basin Washington 7, D. C. Attn: Aerodynamics Laboratory		

DISTRIBUTION LIST

No. of Copies	Organization	No. of Copies	Organization
1	National Advisory Committee for Aeronautics Lewis Flight Propulsion Lab. Cleveland Airport Cleveland, Ohio Attn: F. K. Moore	2	Director, JPL Ord Corps Installation 4800 Oak Grove Drive Department of the Army Pasadena, California Attn: Mr. Irl E. Newlan, Reports Group
2	U. S. Atomic Energy Commission Sandia Corporation P. O. Box 5800 Albuquerque, New Mexico Attn: Mr. Wynne K. Cox	1	Director, Operations Research Office Department of the Army 7100 Connecticut Avenue Chevy Chase, Maryland Washington 15, D. C.
5	Director Armed Services Technical Information Agency Documents Service Center Knott Building Dayton 2, Ohio Attn: DSC - SA	1	Aerophysics Development Corporation P. O. Box 657, Pacific Palisades, California Attn: Dr. William Bollay
1	Commanding General Redstone Arsenal Huntsville, Alabama Attn: Technical Library	2	Applied Physics Lab. 8621 Georgia Avenue Silver Spring, Maryland Attn: Mr. George L. Seielstad
1	Commanding General Frankford Arsenal Philadelphia, Pennsylvania Attn: Reports Group	1	Consolidated Vultee Aircraft Corporation Ordnance Aerophysics Lab. Daingerfield, Texas Attn: Mr. J. E. Arnold
3	Commanding General Picatinny Arsenal Dover, New Jersey Attn: Samuel Feltman, Ammunition Labs. Engineering Research Division Mr. W. R. Benson	1	California Institute of Technology Guggenheim Aeronautical Lab. Passadena, California Attn: Prof. H. W. Liepman
1	Commanding Officer Detroit Arsenal Center Line, Michigan Attn: ORDMX - ECWC	1	Cornell Aeronautical Lab., Inc. 4455 Genesee Street Buffalo, New York Attn: Miss Elma T. Evans Librarian

DISTRIBUTION LIST

No. of Copies	Organization	No. of Copies	Organization
1	California Institute of Tech. Pasadena, California Attn: Library	1	Dr. A. E. Puckett Hughes Aircraft Co. Florence Ave. at Teal St. Culver City, California

1	Goodyear Aircraft Corp.
	Aerophysics Department
	Akron 15, Ohio
	Attn: D. Rohner
	        J. Rudolph
		1	Dr. L. H. Thomas
			Watson Scientific Computing
			  Laboratory
			612 West 116th Street
			New York 27, New York

1	General Electric Company 1 River Road Schenectady, New York Attn: Mr. J. C. Hoffman		

2	Massachusetts Institute of
	  Technology
	Cambridge 39, Massachusetts
	Attn: Guided Missiles Library
	        Room 22-001		

1	North Carolina State College Department of Mathematics Raleigh, North Carolina Attn: Professor John Cell		
1	University of Michigan Willow Run Research Center Willow Run Airport Ypsilanti, Michigan Attn: Mr. J. E. Corey		
3	University of Alabama Tuscaloosa, Alabama Attn: Professor C. L. Seebeck, Jr.		
1	Professor George Carrier Division of Applied Sciences Harvard University Cambridge 38, Massachusetts		
1	Dr. C. B. Millikan Guggen Heim Aeronautical Lab. California Institute of Tech. Pasadena, California		